



# Strength and Durability of Concrete Containing Ceramic Waste Powder and Blast Furnace Slag

Amir AlArab<sup>1</sup>; Bilal Hamad, M.ASCE<sup>2</sup>; and Joseph J. Assaad, M.ASCE<sup>3</sup>

**Abstract:** The replacement rates of portland cement by ceramic waste powder (CWP) are generally limited to few percentages (i.e., less than 10%), as increased additions lead to inferior concrete strength and durability. This paper assesses the importance of blending CWP with blast furnace slag (BFS) to foster synergistic pozzolanic reactions and reinstate strength development despite increased cement replacement rates. Tested binders contained different cement-CWP-BFS proportions, while the evaluated properties included the compressive, splitting tensile, and flexural strengths in addition to the modulus of elasticity, freeze/thaw resistance, and thermal transmittance. Test results showed that concrete strength and durability gradually degraded when the cement was partially replaced by 10%–20% CWP, given the dilution effect that alters hydration reactions and overall porosity. Yet, the concrete properties significantly improved when the CWP and BFS materials were both incorporated in the same binder, indicating the occurrence of synergistic pozzolanic reactions that refined the matrix microstructure. Hence, concrete prepared with ternary binder containing 50% cement, 15% CWP, and 35% BFS exhibited durability and strength properties at 56 days comparable to the control mix made with 100% cement. DOI: [10.1061/\(ASCE\)MT.1943-5533.0004031](https://doi.org/10.1061/(ASCE)MT.1943-5533.0004031). © 2021 American Society of Civil Engineers.

**Author keywords:** Blast furnace slag (BFS); Ceramic waste powder (CWP); Compressive strength; Durability; Freeze and thaw; Sustainability.

## Introduction

The use of powder wastes or by-products rich in siliceous and/or aluminous compounds considerably increased during portland cement production (Malhotra 2000; Assaad and Issa 2017; Abdollahnejad et al. 2019). Such practices proved vital to improve sustainability without impairing the performance and durability of concrete structures. Ceramic waste powders (CWPs) are among those materials abundantly generated during the manufacturing of ceramics used in sanitary, tiling, and refractory works (Singh and Srivastava 2018). It is estimated that about 30% of the daily produced tiles consist of CWP, cumulating globally about 22 billion tons per year (Dieb et al. 2018). If improperly landfilled, CWPs could degrade the soil fertility and groundwater due to leaching of toxic metals such as barium, copper, and cadmium (Dieb et al. 2018).

The use of CWP as partial or complete replacement of natural fine aggregates is well accepted in the concrete industry (Silva et al. 2010; Assaad 2017; Hwalla et al. 2020). Nevertheless, the siliceous nature of such wastes evoked higher interest to assess suitability as

cement substitutes, thus increasing their added-value while reducing the cement carbon footprint. Earlier studies showed that finely ground CWP to less than sieve No. 200 (i.e., 75  $\mu\text{m}$ ) leads to higher strength development, which can be attributed to a microfiller effect coupled with pozzolanic reactions that promote the growth of calcium silicate hydrates (CSH) (Ay and Unal 2000; Lavat et al. 2009; Nayana and Rakesh 2018; Aly et al. 2019). Steiner et al. (2015) found that the calcium hydroxide (CH) content reduced with CWP additions having an average particle size of 9  $\mu\text{m}$ , which led to higher 28-days strength and only 5% mass loss when heated up to 1,000°C. Similar results are reported by Ay and Unal (2000) and Kannan et al. (2017), who demonstrated the pozzolanic properties of CWPs, making them complying to all current physicochemical ASTM C618 (ASTM 2019a) requirements. Naceri and Hamina (2009) showed that grinding CWP with clinker and gypsum increased the late pozzolanic reactivity. Lasseguette et al. (2019) evaluated the hardened properties of mortars containing CWP derived from red and white ceramics, which were ground to 30- $\mu\text{m}$  maximum size and incorporated up to 30% cement replacement. The authors confirmed the occurrence of a secondary hydration reaction that increased the CSH compounds (Lasseguette et al. 2019). The white CWP was found more reactive than the red one, which was attributed to differences in chemical and mineralogical compositions. Lavat et al. (2009) explained that ceramic glazing and color had negligible effect on the pozzolanic reactivity of the powder ground to 45- $\mu\text{m}$  size.

The CWP addition rates have direct influence on strength development and durability of cementitious composites. Raval et al. (2013) indicated that 10%–50% replacements of cement by CWP decreased the concrete 28-days compressive strength ( $f'c$ ) by 7%–40%. Subasi et al. (2017) showed that  $f'c$  drops by 8%–18% with 15% CWP additions, which were ground using a Los Angeles abrasion machine and sieved finer than 125- $\mu\text{m}$ . The scanning electron microscope (SEM) images showed rough and angular-shaped morphology for tested CWP particles (Subasi et al. 2017). Heidari and Tavakoli (2013) reported that cement

<sup>1</sup>Graduate Student, Dept. of Civil and Environmental Engineering, American Univ. of Beirut, P.O. Box 11-0236, Riad ElSolh, Beirut, Lebanon. ORCID: <https://orcid.org/0000-0003-1264-1078>. Email: [ara35@mail.aub.edu](mailto:ara35@mail.aub.edu)

<sup>2</sup>Professor, Dept. of Civil and Environmental Engineering, American Univ. of Beirut, P.O. Box 11-0236, Riad ElSolh, Beirut, Lebanon (corresponding author). Email: [bhamad@aub.edu.lb](mailto:bhamad@aub.edu.lb)

<sup>3</sup>Professor and Chairperson, Dept. of Civil and Environmental Engineering, Univ. of Balamand, Al Kurah, P.O. Box 100, Tripoli, Lebanon. ORCID: <https://orcid.org/0000-0002-2423-451X>. Email: [joseph.assaad@balamand.edu.lb](mailto:joseph.assaad@balamand.edu.lb)

Note. This manuscript was submitted on January 3, 2021; approved on May 13, 2021; published online on October 25, 2021. Discussion period open until March 25, 2022; separate discussions must be submitted for individual papers. This paper is part of the *Journal of Materials in Civil Engineering*, © ASCE, ISSN 0899-1561.

substitution by 10% CWP leads to comparable compressive and flexural strength at 90 days. Vejmelková et al. (2012) showed that the mechanical and transport properties are marginally affected by CWP added up to 20% rates; yet, the fracture energy and chemical resistance to HCl, MgCl<sub>2</sub>, and Na<sub>2</sub>SO<sub>4</sub> can be maintained up to 40%. The fineness level and SiO<sub>2</sub> content in tested CWP were 335 m<sup>2</sup>/kg and 63.5%, respectively. Mohit and Sharifi (2019) investigated the thermal properties of mortars containing up to 25% CWP having 550 m<sup>2</sup>/kg surface area. The authors concluded that such additions enhanced the  $f'c$  and flexural strength of specimens exposed up to 800°C. The SEM images showed reduced open porosity and denser microstructure due to CH conversions into rigid calcium hydrate gels. Dieb and Kannan (2018) developed a performance index to optimize the desired CWP replacement level, recommending 10%–20% CWP rates for strength improvement and workability retention, and 30%–40% rates for optimized durability. Pacheco-Torgal and Jalali (2010) indicated that CWP enhanced the resistance against chloride penetration, however, exhibited higher oxygen permeability and water absorption. The tested concrete was prepared with 20% CWP as partial cement replacement and fixed water-to-binder ratio of 0.6.

Limited investigations evaluated the synergistic effects that could result from blending cement, CWP, and other cementitious materials such as silica fume and blast furnace slag (BFS) on the pozzolanic activity and development of concrete strengths. In fact, the foregoing literature shows that the mechanical and durability-related properties remarkably degrade when the CWP addition rates exceed approximately 10% (Dieb and Kannan 2018; Siddique et al. 2018; Abdollahnejad et al. 2019; Kuan et al. 2020). Therefore, the exploration of possible synergistic effects to foster pozzolanic reactions can be of particular interest to highlight the CWP benefits as value-added pozzolan, thus increasing the cement substitution rates and leading to improved sustainability.

Heidari and Tavakoli (2013) studied the importance of synergistic effects by combining CWP and glassy nano-SiO<sub>2</sub> particles to promote the growth of CSH compounds through pozzolanic reactions. The CWP was obtained by grinding ceramics finer than sieve No. 200 (i.e., fineness of 340 m<sup>2</sup>/kg), while the fineness and silica content of the nano-SiO<sub>2</sub> were 2,000 m<sup>2</sup>/kg and more than 99.8%, respectively. The authors reported that a 15%–0.5% CWP-SiO<sub>2</sub> combination could overcome the deficiency in  $f'c$  at all ages, while mixtures containing CWP-SiO<sub>2</sub> of 20%–1% were required to secure equivalent strengths. Recently, AlArab et al. (2020) proved through physicochemical characterization the synergistic benefits on the pozzolanic activity that could emanate from blending cement, CWP, and BFS materials. The results were corroborated by SEM images as well as using the Frattini, X-ray diffraction, and thermogravimetric testing performed at various ages. Mortars prepared using ternary binders containing 50% cement together with 20% CWP and 30% BFS exhibited higher strengths than mixtures containing 80% cement and 20% CWP (or, also, mixtures containing 80% cement and 20% BFS). The ternary binder mortars exhibited improved the residual  $f'c$  at elevated temperatures up to 800°C.

This paper is the continuation of a previous work undertaken to assess the benefits of combining CWP and BFS in cementitious materials (AlArab et al. 2020). It mainly seeks to validate the synergistic pozzolanic reactions observed on paste and mortar mixtures to enhance the concrete strength and durability-related properties. A relatively low to high water-to-binder ratio (w/b) of 0.27 and 0.54 are considered, while different binders containing up to 20% CWP and 40% BFS replacement rates are tested. The evaluated properties determined after 7, 28, and 56 days included the  $f'c$ , splitting tensile and flexural strengths, modulus of elasticity, freeze/thaw resistance, and thermal transmittance. The findings of

this work would help reducing the harmful environmental effects associated with the indiscriminate dumping of CWP as well as decreasing the volume of portland cement used in concrete production.

## Experimental Program

### Binder Components and Proportions

Commercially available cement designated as CEM II/B-L and BFS conforming respectively to BS EN 197-1 (CEN 2011) and ASTM C989 Grade 80 (ASTM 2018a) requirements are used. Their specific gravities are 3.15 and 2.6, respectively, while the Brunauer–Emmett–Teller (B.E.T.) surface areas are 515 and 770 m<sup>2</sup>/kg, respectively (Table 1). The CWP was derived from porcelain tiles that are crushed using a jaw crusher to pieces smaller than 10 mm, then ground using a bico-pulverizer to produce a fine powder whose 95% particles are finer than sieve No. 200. As given in Table 1, the CWP had a surface area and porosity of 365 m<sup>2</sup>/kg and 22.4%, respectively, making it much coarser and porous than the cement and BFS materials. The porosity was determined on dry powders, as per ISO 9277 (ISO 2010), which consists of exposing the materials to nitrogen gas at different pressure conditions and measuring the weight uptake and monolayer capacity. The CWP is rich in SiO<sub>2</sub> and Al<sub>2</sub>O<sub>3</sub> compounds, with excellent resistance to heat (i.e., mass loss is nil at 1,000°C). The mass loss increased to 4.9% and 9.7% for the cement and BFS, respectively, mostly as a result of CaO decomposition at temperatures varying from 600°C to 800°C (Mehta and Monteiro 2006; Lubloy et al. 2016).

Prior to concrete batching, a series of preliminary mortar tests were performed to select the binder proportions including the upper cement substitution limits by BFS or CWP materials. Those limits were considered to be reached when the 28-days strength activity index (SAI) drops below the recommended range that varies within 85%–95% according to ASTM C989 (ASTM 2018a). Testing was realized by gradually replacing the cement by CWP (or BFS), while the binder-to-sand-to-water ratio was set at 1:2.75:0.5 [ASTM C311 (ASTM 2018c)]. Results showed that the CWP and BFS replacement rates should not exceed 20% or 40%, respectively; otherwise, the SAI will drop significantly below the ASTM C989 limitation.

### Concrete Materials, Proportions, and Mixing

The fine aggregates (i.e., sand) had a fineness modulus of 3, specific gravity of 2.64, and absorption capacity of 0.6%. A 19-mm

**Table 1.** Chemical and physical properties of the powders used

Oxides/minerals/properties	Cement	BFS	CWP
CaO (%)	66.6	42.1	2.3
SiO <sub>2</sub> (%)	21.5	32.6	67.3
Al <sub>2</sub> O <sub>3</sub> (%)	4.6	12.2	19.8
Fe <sub>2</sub> O <sub>3</sub> (%)	2.8	0.55	2.5
MgO (%)	1.2	5.45	2
SO <sub>3</sub> (%)	2.7	4	0.1
C <sub>3</sub> S (%)	65.1	N/A	N/A
C <sub>2</sub> S (%)	12.7	N/A	N/A
C <sub>3</sub> A (%)	7.5	N/A	N/A
C <sub>4</sub> AF (%)	8.5	N/A	N/A
Loss on ignition (LOI) (%)	3	2	0
Specific gravity	3.15	2.6	2.65
B.E.T. surface area (m <sup>2</sup> /kg)	515	770	365
Residual mass loss at 1,000°C (%)	9.7	3.9	0
Porosity (%)	4.3	18.3	22.4

**Table 2.** Binder composition and  $f'c$  at various ages

Mix codification	Cement (kg/m <sup>3</sup> )	BFS (kg/m <sup>3</sup> )	CWP (kg/m <sup>3</sup> )	w/b	7-day $f'c$ (MPa)	28-day $f'c^a$ (MPa)	56-day $f'c$ (MPa)
0.54-CEM100	370	0	0	0.54	21.3	30.6 (1.7)	33.4
0.54-CEM90/CWP10	333	0	37	0.54	17.4	26.8 (1.1)	30.5
0.54-CEM85/CWP15	314.5	0	55.5	0.54	15.6	23.9 (2)	26.3
0.54-CEM80/CWP20	296	0	74	0.54	14.6	18.8	23.3
0.54-CEM60/BFS40	222	148	0	0.54	19.3	31.2 (4.5)	39.4
0.54-CEM55/BFS35/CWP10	203.5	129.5	37	0.54	17.6	29.1 (3)	34.9
0.54-CEM50/BFS35/CWP15	185	129.5	55.5	0.54	16.3	25.2 (1.2)	30.9
0.54-CEM50/BFS30/CWP20	185	111	74	0.54	14.4	21.3	26.9
0.27-CEM60/BFS40	336	224	0	0.27	40.3	56 (2.1)	61.5
0.27-CEM50/BFS35/CWP15	280	196	84	0.27	35.7	52.1 (3.4)	56.7
0.27-CEM50/BFS30/CWP20	280	168	112	0.27	32.4	46.6 (1.7)	50.1

Note: Binder content,  $\text{kg/m}^3 = \sum(\text{Cement} + \text{BFS} + \text{CWP})$ ; for moderate strength concrete (0.54-w/b), the water content, sand, and coarse aggregates were equal to 200, 807, and 991  $\text{kg/m}^3$ , respectively; and for high strength concrete (0.27-w/b), the water content, sand, and coarse aggregates were equal to 150, 772, and 960  $\text{kg/m}^3$ , respectively.

<sup>a</sup>Values between parenthesis refer to the coefficient of variation (COV) (%).

maximum size coarse aggregate was used; its dry unit weight, specific gravity, and absorption capacity were 1,600  $\text{kg/m}^3$ , 2.68, and 1.74%, respectively. The gradation curves of the fine and coarse aggregates comply with ASTM C33 (ASTM 2003) requirements. A naphthalene-based water-reducing (WR) admixture was employed; its specific gravity and solid content were 1.18 and 35%, respectively.

Two concrete series proportioned to exhibit relatively moderate to high  $f'c$  values are tested, allowing wider assessment of CWP and BFS effects on pozzolanic reactions and strength development. The binder content varied from 370 to 560  $\text{kg/m}^3$ , while the corresponding w/b was 0.54 and 0.27, respectively. As provided in Table 2, the control mix in the moderate strength concrete series was prepared with only cement, while this was gradually substituted on mass basis by 10%, 15%, and 20% CWP in the other mixtures. The cement content decreased to 60% when the BFS materials are incorporated, given the satisfactory SAI values obtained at such replacement rates [ASTM C989 (ASTM 2018a)]. Subsequently, three binder proportions composed of 50%–55% cement, 30%–35% BFS, and 10%–20% CWP materials were considered, in order to assess the synergistic effects that could result from such additions. The fine-to-total coarse aggregate ratio remained fixed at 0.45, while the WR was incorporated at 0.6%, by mass of binder, to achieve a slump hovering about 180  $\pm$  40 mm. The mixture codification refers to w/b and cement/BFS/CWP percent content in the binder used.

The binder of the control high-strength concrete was composed of 60% cement and 40% BFS (Table 2). In fact, the use of only cement at such a high content of 560  $\text{kg/m}^3$  is not a sustainable practice, but also could detrimentally alter concrete durability due to excessive heat increase during hydration reactions (Assaad and Issa 2014; Matar and Assaad 2019). Two binder proportions containing 50% cement along with 30%–35% BFS and 15%–20% CWP materials are investigated. As earlier, the fine-to-total coarse aggregate ratio remained at 0.45, while the WR was adjusted at 1.2%, by mass of binder.

The mixing process consisted of homogenizing the fine and coarse aggregates together with half of mixing water for about 1 min. The binder (i.e., cement, CWP, and BFS) was then introduced, followed by the remaining mixing water and WR. The concrete was mixed for 2 min, followed by a resting period of 30 s, before resuming for an additional 1 min. Testing and sampling were conducted at room temperature of  $22^\circ\text{C} \pm 3^\circ\text{C}$  and relative humidity of  $60\% \pm 10\%$ .

### Testing Methods and Procedures

Right after mixing, the slump and fresh concrete density were determined according to ASTM C143 (ASTM 2015c) and C138 (ASTM 2017a) test methods, respectively. The concrete is filled in  $100 \times 200$  mm steel cylinders to determine the  $f'c$  and splitting tensile strength ( $f_t$ ) according to ASTM C39 (ASTM 2015a) and C496 (ASTM 2011), respectively. The modulus of elasticity ( $E$ ) was measured using  $150 \times 300$  mm cylinders according to ASTM C469 (ASTM 2014). The cylinders used for  $f'c$  and  $E$  measurements were capped with sulfur, as specified in ASTM C617 (ASTM 2012), and tested at a deformation rate of 1.25 mm/min. All specimens were demolded after 24 h, and moist cured at 95% relative humidity and  $22^\circ\text{C} \pm 3^\circ\text{C}$  ambient temperature. The compressive strength was realized after 7, 28, and 56 days in order to better assess the occurrence of pozzolanic reactions and strength development over time. An average of three values was considered in this study, and the mean values are reported in Tables 2 and 3.

The flexural strength ( $f_r$ ) was determined using  $150 \times 150 \times 500$  mm beams by third-point bending, as per ASTM C78 (ASTM 2018b), while recording the midspan deflection using an LVDT. The flexural toughness index ( $T$ ) was deduced from the area under the load versus deflection curves at the failure state. The concrete resistance to freezing and thawing was determined after 56 days using  $75 \times 100 \times 405$  mm specimens [ASTM C666 (ASTM 2015b)]. Testing was performed underwater up to 150 cycles; each cycle consisted of fluctuating the temperature from  $4^\circ\text{C}$  to  $-8^\circ\text{C}$ , and vice versa. The fundamental transverse frequency was determined after a given number of cycles using a resonance tester according to ASTM C215 (ASTM 2019b). The relative dynamic modulus of elasticity (RDME) was calculated as:  $\text{RDME, \%} = (n^2/n_i^2) \times 100$ , where  $n_i$  and  $n$  refer to the fundamental transverse frequency measured in the initial state and after a given number of freeze/thaw cycles, respectively. Two replicates were tested for each mixture to determine the average flexural strength and RDME responses (Tables 3 and 4).

The concrete thermal transmittance (R-value) was determined after 56 days using a steady state one-dimensional heat flux conductivity apparatus according to ASTM C518 (ASTM 2017b). The  $300 \times 300 \times 25$  mm blocks were properly molded to ensure smooth contact surfaces, and edge insulation was implemented to control the heat losses. The hot plate beneath the specimen was regulated at  $40^\circ\text{C}$ , and the Fourier's law of heat conduction was used to calculate the R-value. The steady state condition was

**Table 3.** Hardened mechanical properties of investigated mixtures

Mix codification	$f_t$ (MPa)		$f_r$ (MPa)		Toughness, $T$ (J)		$E$ (GPa)	
	28-day	56-day	28-day	56-day	28-day	56-day	7-day	28-day
0.54-CEM100	2.59 (0.7)	2.86 (1.5)	4.9	5.18	5.01	5.14	16.7 (3)	19.9
0.54-CEM90/CWP10	2.49 (3.1)	2.49 (0.8)	4.28	5.01	4.08	4.93	15.6	19.5
0.54-CEM85/CWP15	2.35 (2)	2.63 (3.1)	4.32	4.93	4.18	4.21	13.2	18.2
0.54-CEM80/CWP20	2.32	2.63 (2.1)	4.15	4.26	5.97	2.77	13.3	16.7
0.54-CEM60/BFS40	2.79	3.18 (4.1)	5.58	6.31	5.51	5.63	18.9 (4.5)	23.6
0.54-CEM55/BFS35/CWP10	2.67 (1.3)	3.12	4.67	5.48	3.2	4.3	18.8 (1.1)	21.2
0.54-CEM50/BFS35/CWP15	2.58 (2.2)	3.02	4.44	6.01	3.31	4.76	15.1 (0.7)	19.3
0.54-CEM50/BFS30/CWP20	2.57	2.69	4.57	5.45	3.76	4.4	13.8 (2.4)	18.7
0.27-CEM60/BFS40	4.28 (1.1)	5.01	8.56	8.7	7.14	8.95	26.4 (6.1)	31.8
0.27-CEM50/BFS35/CWP15	4.01 (3)	4.55	8.07	8.57	6.77	7.35	23.5 (5.1)	28.6
0.27-CEM50/BFS30/CWP20	4.11 (2.8)	4.18	7.11	7.81	6.79	6.59	21.5	26.7

Note: Values between parenthesis refer to the COV (%).

**Table 4.** RDME measurements after given number of freeze/thaw cycles

Mix codification	After 30 cycles	After 60 cycles	After 90 cycles	After 120 cycles	After 150 cycles
0.54-CEM100	90	90	90	86	86
0.54-CEM90/CWP10	86	77	68	68	64
0.54-CEM85/CWP15	86	69	65	50	47
0.54-CEM80/CWP20	66	54	50	38	30
0.54-CEM60/BFS40	100	91	91	86	82
0.54-CEM55/BFS35/CWP10	87	83	79	73	67
0.54-CEM50/BFS35/CWP15	95	78	78	59	59
0.54-CEM50/BFS30/CWP20	91	91	87	69	57
0.27-CEM50/BFS35/CWP15	96	96	96	96	96
0.27-CEM50/BFS30/CWP20	95	95	95	95	91

reached when no more than 1% mass loss was recorded over a 24 h period.

## Results and Discussion

The accuracy of various responses were determined when repeating the same batch three times; the coefficient of variation (COV) was calculated as the ratio between the mean of different values divided by the standard deviation, multiplied by 100. As provided in Tables 2 and 3, the COV values varied within 0.7%–4.5%, reflecting good repeatability. The highest COV of 5.1% and 6.1% corresponded to  $E$  measurements for the 0.27-w/b mixtures prepared with CEM60/BFS40 and CEM50/BFS35/CWP15 binders.

### Compressive and Splitting Tensile Strengths

The  $f'_c$  values determined after 28 and 56 days for the mixtures prepared with 370 kg/m<sup>3</sup> binder are plotted in Fig. 1; the ratio of  $f'_c$  recorded after 56 and 7 days is also shown. Regardless of testing age, the incorporation of CWP as partial cement replacement gradually reduced  $f'_c$ ; for example, this decreased from 30.6 MPa for the control CEM100 mixture to 26.8 and 18.8 MPa with 10% and 20% CWP additions, respectively. The corresponding  $f_t$  decreased from 2.59 to 2.49 and 2.32 MPa, respectively (Table 3). This can naturally be attributed to a dilution effect resulting from the cement substitution by CWP, leading to reduced hydration activity that detrimentally alters microstructure and formation of CSH compounds (Dieb et al. 2018; ElMir et al. 2020). Concurrently, the CWP particles are characterized by higher porosity (i.e., 22.4% versus 4.3% for the cement), which could degrade the concrete stiffness and capacity to resist compression or tensile loading

(Silva et al. 2016). This phenomenon is further aggravated by the CWP coarse particles (365 m<sup>2</sup>/kg versus 515 m<sup>2</sup>/kg for the cement) that reduce the microfiller effect and packing density in the cementitious system (Khayat et al. 2003; Knop and Peled 2018).

Although the  $f'_c$  and  $f_t$  magnitudes curtailed with CWP additions, the rates of strength increase over time were higher than those of the control mix. Hence, for example, the  $f'_c(56 \text{ day})/f'_c(7 \text{ day})$  ratio increased from 1.57 for the control CEM100 binder to 1.75 and 1.69 for the CEM90/CWP10 and CEM85/CWP15 binders, respectively (Fig. 1). This physically reflects the pozzolanic nature of such additions and their efficiency to promote the conversion of CH to CSH compounds, leading to increased strength development. This finding was corroborated by the Frattini tests and x-ray diffraction (XRD) analysis (AlArab et al. 2020; Siddique et al. 2018), which was directly attributed to the CWP chemical composition that affects hydration reactions and phase assemblage. The binder containing 20% CWP exhibited an  $f'_c(56 \text{ day})/f'_c(7 \text{ day})$  ratio of 1.6 (i.e., close to the control mix), which may be due to the high CWP content in the produced binder.

The 28-days  $f'_c$  for the concrete prepared using CEM60/BFS40 binder was close to the control mix (i.e., 31.2 MPa), which then remarkably increased to register the highest value of 39.4 MPa after 56 days (Fig. 1); the resulting  $f'_c(56 \text{ day})/f'_c(7 \text{ day})$  ratio reached 2.04. This can be directly related to the amorphous calcium aluminosilicate nature of the BFS materials, which are known by their capacity to exhibit both pozzolanic and latent hydration activities (Mehta and Monteiro 2006; Hou et al. 2018), especially when having a high fineness level of 770 m<sup>2</sup>/kg. The corresponding  $f_t$  responses were 2.79 and 3.18 MPa after 28 and 56 days, respectively, making them also the highest values recorded for the mixtures made using 370 kg/m<sup>3</sup> binder content (Table 3).

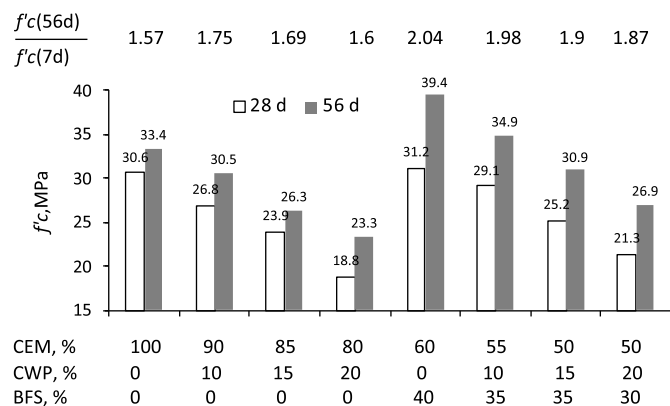


**Fig. 1.** Effect of binder composition on  $f'c$  variations for moderate strength concrete.

The incorporation of CWP in the CEM/BFS binder led to gradual decrease in  $f'c$  and  $ft$  values, just like what happened when the cement was only used (Fig. 1). Hence, the 28-days  $f'c$  decreased to 29.1 and 21.3 MPa when 10% and 20% CWP are respectively introduced, while the corresponding  $ft$  decreased to 2.67 and 2.57 MPa. As earlier explained, this can be attributed to the dilution effect in addition to the coarse and porous natures of the CWP materials. Nevertheless, two peculiar observations should be highlighted; the first relates to the higher 56-days  $f'c$  recorded for the concrete prepared with CEM55/CWP10/BFS35 binder compared to the control mix (i.e., 34.9 versus 33.4 MPa, respectively), and the second relates to the remarkably higher  $f'c(56 \text{ day})/f'c(7 \text{ day})$  ratios that hovered around 1.9 for mixtures prepared using the ternary CEM/BFS/CWP binders. As will be discussed and quantified later in the text, such observations reflect the occurrence of secondary hydration reactions resulting from the synergistic effects of both BFS and CWP materials (Arora et al. 2016; Sujjavanich et al. 2017; AlArab et al. 2020).

The magnitude of  $f'c$  and  $ft$  responses almost doubled for mixtures prepared with 560 kg/m<sup>3</sup> binder and 0.27 w/b (Tables 2 and 3), which can normally be attributed to higher binder content and reduced free water content that can refine the concrete porosity and microstructure (Mehta and Monteiro 2006). Hence, for example, the  $f'c$  reached 56 and 61.5 MPa for the 0.27-CEM60/BFS40 concrete after 28 and 56 days, respectively. Yet, as earlier noticed for the moderate strength concrete, the incorporation of CWP led to reduced strength (i.e., the  $f'c$  dropped to 56.7 and 50.1 MPa after 56 days for the 0.27-w/b mixtures containing 15% and 20% CWP, respectively).

Good relationships with high correlation coefficients ( $R^2$ ) exist between the  $f'c$  and  $ft$  responses for all tested mixtures, as expressed in Eqs. (1) and (2). Also, it is worth noting that the splitting tensile strength can well be predicted from the concrete  $f'c$  using the exponential analytical model [i.e.,  $ft = k(f'c)^n$ ] proposed by ACI 318-19 (ACI 2019), where  $k$  and  $n$  are taken as 0.56 and  $\frac{1}{2}$ , respectively. The resulting coefficient of proportionality between the measured-to-predicted values is 0.95, while the  $R^2$  value is equal to 0.993

$$\text{After 28 days: } ft, \text{ MPa} = 0.0576 (f'c, \text{ MPa}) + 1.085 \quad R^2 = 0.94 \quad (1)$$

$$\text{After 56 days: } ft, \text{ MPa} = 0.0657 (f'c, \text{ MPa}) + 0.834 \quad R^2 = 0.95 \quad (2)$$

### Flexural Strength and Toughness

The load versus deflection curves determined after 28 days for beams prepared with concrete containing 370 kg/m<sup>3</sup> binder are plotted in Fig. 2. As shown, the stiffness of ascending curves as well as the ultimate load at failure reduced with CWP additions, which can mainly be attributed to a dilution effect that weakens the hydrating gel bonds and reduces the development of strength (Dieb et al. 2018; ElMir et al. 2020). Hence, the  $fr$  computed at failure decreased from 4.9 MPa for the control CEM100 concrete

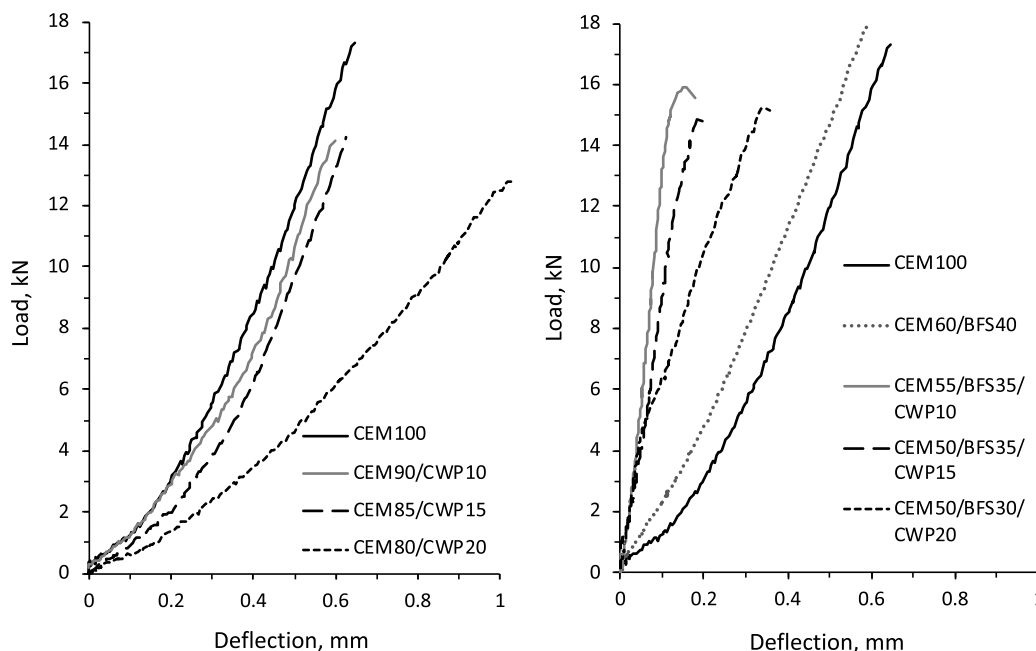


**Fig. 2.** Load versus deflection curves for moderate strength concrete beams.

to 4.28 and 4.32 MPa for the CEM90/CWP10 and CEM85/CWP15 mixtures, respectively (Table 3). The corresponding toughness ( $T$ ) decreased from 5.01 to 4.08 and 4.18 J, respectively. On the other hand, as noted earlier, the porous CWP particles may contribute to reduced concrete stiffness and lead to larger deflections for a given load (Silva et al. 2010; Dieb and Kanaan 2018). This was particularly noticed for the CEM80/CWP20 concrete specimen that experienced significant deflections reaching around 1 mm at the ultimate load (Fig. 2).

The concrete prepared with the CEM60/BFS40 binder exhibited the highest  $fr$  and  $T$  responses among the moderate strength mixtures, reaching 6.31 MPa and 5.63 J after 56 days (Fig. 3). Such results are in line with  $f'c$  measurements, reflecting the pozzolanic and latent hydration activities of the BFS materials (Shi 2004; Schuldyakov et al. 2016). Nevertheless, as shown in Fig. 2, the drop in ultimate load due to CWP additions was accompanied with reduced deflections reflecting increased brittleness of tested beams. Hence, mixtures made with the ternary binders exhibited the lowest  $T$  values, hovering about  $4.5 \pm 0.25$  J after 56 days, which most likely could be associated to a refined and denser pore system achieved through synergistic hydration reactions. This analysis is consistent with the significant increase in the  $fr(56 \text{ day})/fr(28 \text{ day})$  ratios that reached 1.35 for the CEM50/BFS35/CWP15 mixture (Fig. 3). Earlier studies showed that the bending strength is largely dictated by the length of largest pores, as given in the Griffith model, with direct consequences on toughness, elastic modulus, and fracture energy (Jivkrov et al. 2013; Liu et al. 2017).

Schlangen and Qian (2009) reported that the brittleness of cement pastes increases when the large pores and internal defects are removed from the cement paste.

As expected, the  $fr$  responses for mixtures containing  $560 \text{ kg/m}^3$  CEM60/BFS40 binder reached 8.7 MPa after 56 days, but then decreased to 8.57 and 7.81 MPa with the addition of 15% and 20% CWP, respectively. The corresponding  $T$  varied from 8.95 to 7.35 and 6.59 J, respectively. It is to be noted that good relationships can be established between the flexural and compressive strength properties for all tested mixtures, as expressed in Eqs. (3) and (4). The coefficient of proportionality determined between the measured flexural strength responses and those predicted using the exponential analytical model [i.e.,  $fr = k(f'c)^n$ ] is 1.37, with an  $R^2$  value of 0.988. The  $k$  and  $n$  parameters are taken as 0.7 and  $\frac{1}{2}$ , respectively [ACI 318 (ACI 2019)]

$$\text{After 56 days: } T, J = 1.048 (fr, \text{MPa}) - 1.084 R^2 = 0.88 \quad (3)$$

$$\text{After 56 days: } fr, \text{MPa} = 0.115 (f'c, \text{MPa}) + 1.823 R^2 = 0.94 \quad (4)$$

### Quantification of Synergistic Effects

Fig. 4 plots the normalized strengths [i.e.,  $\Delta(f'c)$ ,  $ft$ , and  $fr$ ] due to CWP and/or BFS additions after 28 and 56 days determined for the 0.54-w/b concrete mixtures. The  $\Delta(\text{Strength})$  is computed as follow:

$$\Delta(\text{Strength}), \% = \left( \frac{\text{Strength of modified concrete} - \text{Strength of control CEM 100 mix}}{\text{Strength of control CEM 100 mix}} \right) \times 100$$

Clearly, the strength responses progressively dropped when the cement is replaced by CWP additions. The highest strength drop occurred during compression testing, which varied  $\Delta(f'c)$  at 28 days from  $-12.4\%$  to  $-21.9\%$  and  $-38.6\%$  at 10%, 15%, and 20% CWP rates, respectively. This can mostly be attributed to the porous CWP nature that reduces concrete stiffness and capacity to resist the high stresses due to compression loading. The tensile and flexural properties were less influenced by such additions; the  $\Delta(ft)$  and  $\Delta(fr)$  reached, respectively,  $-8\%$  and  $-17.8\%$  for

the concrete prepared with 80CEM/20CWP binder. With few exceptions, the  $\Delta(\text{Strength})$  values decreased over time, reflecting higher strength development due to the continued hydration reactions. Hence, for example,  $\Delta(f'c)$  varied from  $-38.6\%$  to  $-30.2\%$  after 28 and 56 days, respectively, for concrete containing the 80CEM/20CWP binder. The corresponding  $\Delta(ft)$  varied from  $-10.4\%$  to  $-8\%$ , respectively.

The concrete made with CEM60/BFS40 binder exhibited positive  $\Delta(\text{Strength})$  values due to the presence of BFS materials (Fig. 4). Yet, the strength gradually degraded when the CWP was introduced in the ternary binder, albeit the resulting  $\Delta(\text{Strength})$  values remained significantly less pronounced compared to mixtures containing only cement and CWP. For instance, at 10% CWP additions, the  $\Delta(f'c)$  switched from  $-4.9\%$  to  $4.5\%$  after 28 and 56 days, respectively, while the corresponding  $\Delta(fr)$  varied from  $-4.7\%$  to  $5.8\%$ . This reflects the occurrence of synergistic pozzolanic reactions resulting from the presence of both CWP and BFS materials, thus promoting the conversion of CH to rigid CSH compounds and leading to higher mechanical properties compared to the control mixture (Sujjavanich et al. 2017; AlArab et al. 2020). As shown in Fig. 5, the SEM images taken after 56 days on hydrated pastes showed some remaining CH crystals in the control paste made with only cement, while the microstructure become much denser and CH crystals less visible in the hybrid binders due to secondary hydration reactions (AlArab et al. 2020). At 15% CWP, the drop in  $f'c$  after 56 days was very small and within the repeatability of testing [i.e.,  $\Delta(f'c)$  equal to  $-7.5\%$ ], while the

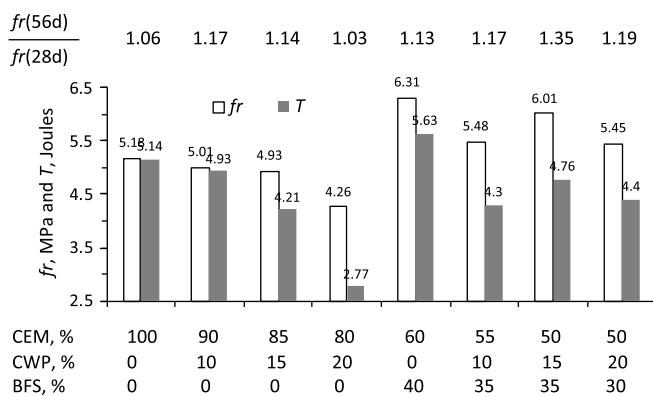


Fig. 3. Effect of binder composition on  $fr$  and  $T$  responses determined after 56 days for the moderate strength concrete.

$\Delta(f_t)$  and  $\Delta(f_r)$  were positive, reflecting higher strengths compared to the control CEM100 mixture. This again reveals the importance of combining both CWP and BFS materials to foster the pozzolanic synergistic effects with improved strength development. From a sustainable point of view, this reflects the relevance of such materials to reduce cement content while increasing the CWP in the

produced binder without impairing the performance and strength of the concrete mixtures.

### Modulus of Elasticity

The effect of CWP and BFS additions on the modulus of elasticity responses determined after 7 and 28 days for the moderate strength mixtures is plotted in Fig. 6. Concurrent with previous findings, the  $E$  measurements gradually decreased when the cement is partially replaced by CWP; for example, this varied from 19.9 GPa after 28 days for the control mixture to 18.2 and 16.7 GPa with 15% and 20% CWP rates, respectively. As explained previously, this can be attributed to the porous CWP nature that decreases concrete stiffness, leading to larger strains for a given load (Naceri and Hamina 2009; Silva et al. 2010). The concrete prepared with CEM60/BFS40 binder exhibited the highest  $E$  of 23.6 GPa, which then gradually decreased when the CWP is introduced in the binder. The  $E$  responses recorded for mixtures made using CEM55/BFS35/CWP10 binder were higher than the control CEM100 concrete (i.e., 21.2 versus 19.9 GPa), due to pozzolanic effects. The  $E$  values reached 31.8 GPa for high strength 0.27-w/b concrete prepared with CEM60/BFS40 binder, which decreased to 26.7 GPa for the 0.27-CEM50/BFS30/CWP20 mixture (Table 3).

Good relationships exist between the modulus of elasticity and concrete  $f'c$  for all tested mixtures, as expressed in Eqs. (5) and (6). The coefficient of proportionality determined between the measured  $E$  responses and those predicted using the exponential analytical model [i.e.,  $E = 4,730(f'c)^n$ ] is 0.84, with an  $R^2$  value of 0.998. The  $n$  parameter is taken as  $\frac{1}{2}$  [ACI 318 (ACI 2019)]

$$\text{After 7 days: } E, \text{ GPa} = 0.446 (f'c, \text{ MPa}) + 7.95 \quad R^2 = 0.89 \quad (5)$$

$$\text{After 28 days: } E, \text{ GPa} = 0.373 (f'c, \text{ MPa}) + 9.93 \quad R^2 = 0.95 \quad (6)$$

### Freeze and Thaw Resistance

Typical RDME plots determined after 60 and 150 freeze/thaw cycles for the moderate strength mixtures are given in Fig. 7. Compared to the 86% value recorded after 150 cycles for the CEM100 control concrete, the incorporation of CWP led to significant decrease in the RDME reaching 64%, 47%, and 30% at 10%, 15%, and 20% CWP rates, respectively. This can be related to a dilution effect that reduces the concrete strength and ability to resist the deteriorating stresses due to freeze/thaw cycles (Siddique et al. 2018; ElMir et al. 2020). Concurrently, it is worth noting that the

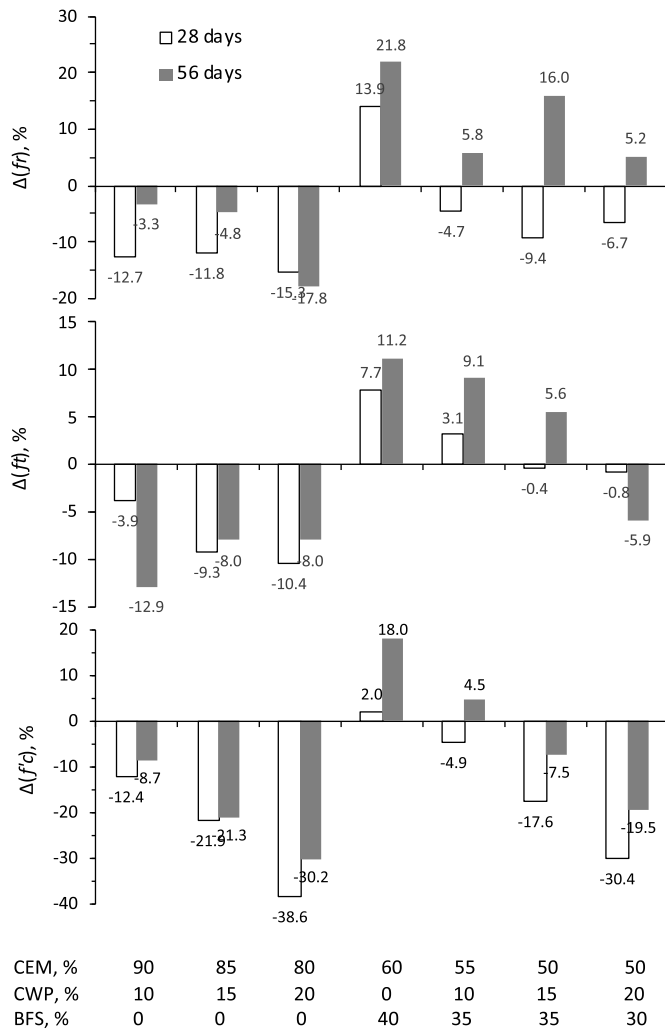


Fig. 4. Strength variations after 28 and 56 days due to BFS and/or CWP additions.

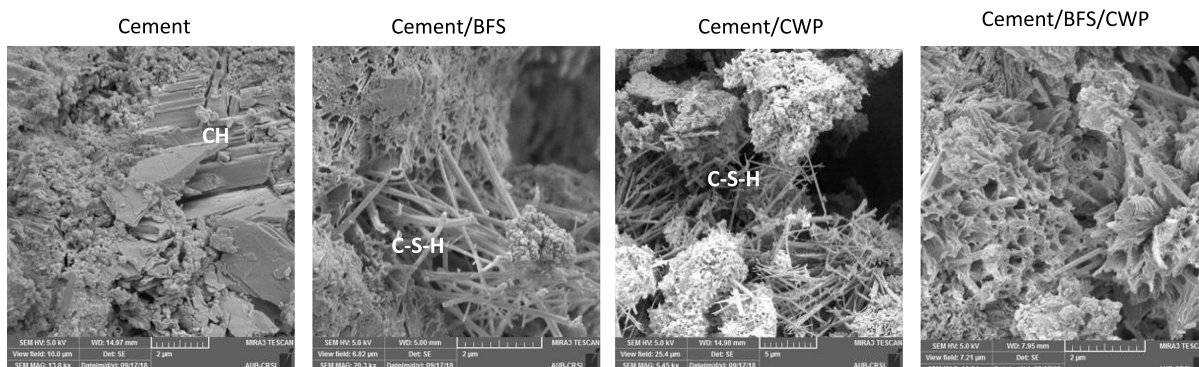
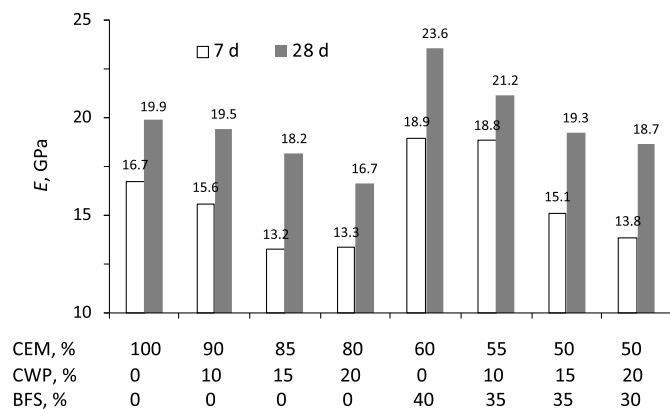
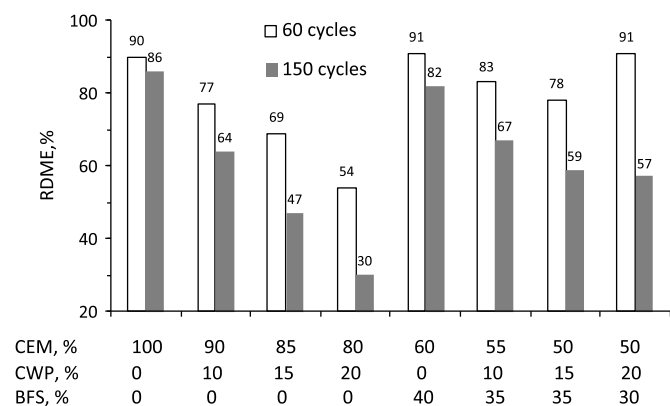


Fig. 5. SEM images of hydrated pastes after 56 days curing.



**Fig. 6.** Effect of binder composition on  $E$  responses after 7 and 28 days for moderate strength concrete.



**Fig. 7.** Effect of binder composition on RDME after 60 and 150 cycles for moderate strength concrete.

CWP's porous nature may have favored water penetration inside the particles, which under freezing conditions could increase the concrete vulnerability to cracking and delamination of constituent bonds (Deja 2003; Kuan et al. 2020). Fig. 8 shows how one of the 20% CWP replicates broke completely after 150 cycles. This specimen did not only experience pop-outs but also complete disruption of the paste reaching the upper surface, which caused its rupture. These findings indicate the harmful impact of high CWP rates on concrete durability, which is line with the study reported by Vejmelková et al. (2012).

The concrete made using CEM60/BFS40 binder behaved almost similar to the control specimen; the RDME values were pretty close to each other (Fig. 7). The resistance to freeze/thaw cycles gradually curtailed with the incorporation of CWP in the ternary binders, albeit the resulting RDME values were higher than those registered for mixtures made with only cement. Hence, the RDME recorded after 150 cycles were 59% and 57% for mixtures prepared with CEM50/BFS35/CWP15 and CEM50/BFS30/CWP20 binders, respectively. Such results are in agreement with previous strength data (i.e.,  $f'c$ ,  $ft$ , and  $fr$ ), confirming the beneficial effects of BFS and CWP materials on the synergistic pozzolanic reactions that strengthen the concrete microstructure and improve durability. As shown in Fig. 8, the exterior surfaces for specimens made with 560 kg/m<sup>3</sup> binder remained almost intact after 150 cycles, given their dense microstructure associated with the reduced w/b to 0.27. The resulting RDME values were higher

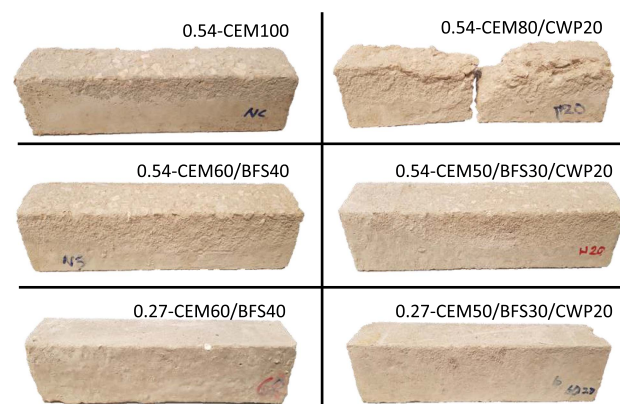


**Fig. 8.** Photos for tested concrete beams after 150 freeze/thaw cycles.

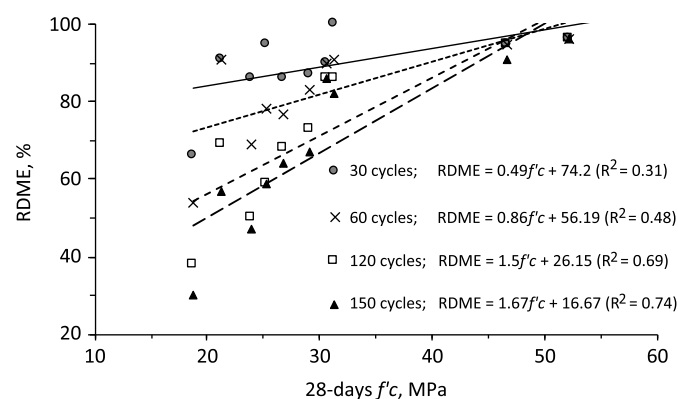


**Fig. 9.** Relationships between 28-days  $f'c$  and RDME measurements after different number of cycles.

than 91% (Table 4), reflecting excellent resistance to freeze/thaw cycles.

Fig. 9 plots the relationships between the 28-days  $f'c$  with respect to RDME values recorded after different cycles for all tested concrete (interestingly, the  $R^2$  values gradually improved from 0.31 to 0.74 with the number of testing cycles). Clearly, mixtures exhibiting higher  $f'c$  are shown to better resist freeze/thaw cycles, leading to increased RDME measurements.

### Thermal Transmittance

As shown in Fig. 10, the R-value remained within the repeatability of testing (i.e., from 0.53 to 0.57 m<sup>2</sup> · K/W) for mixtures prepared with CEM100 and CEM85/CWP15 binders. Yet, this remarkably improved to 0.79 m<sup>2</sup> · K/W when 40% BFS materials were incorporated in the binder, given the refractory nature and chemical composition (mostly MgO) of such additions that are known by their efficiency to improve the thermal properties (Grubesa et al. 2016; Jabri et al. 2018). On the other hand, concrete prepared with 0.27-w/b exhibited significantly reduced R-value, dropping down to 0.32 and 0.35 m<sup>2</sup> · K/W for CEM60/BFS40 and CEM50/BFS35/CWP15 mixtures, respectively. Such results are consistent with the reduced w/b that refines microstructure and decreases porosity of high strength concrete mixtures, leading to increased heat conductivity and reduced thermal transmittance (Aydin 2008; Quanlin et al. 2002).

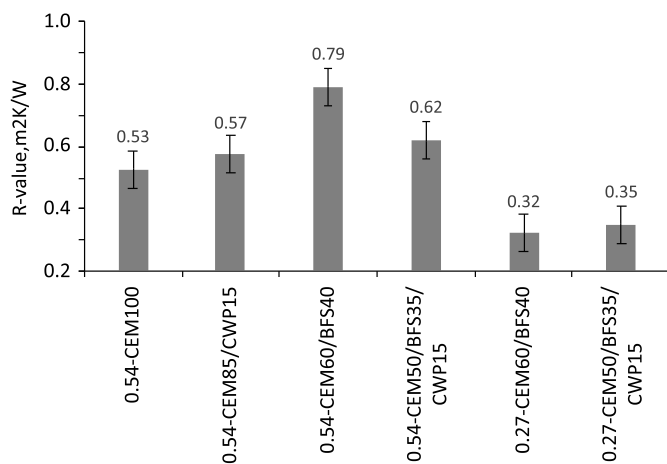


**Fig. 10.** Effect of binder composition on R-values determined after 28 days.

## Summary and Conclusions

Generally, the cement replacement rates by CWP are limited to few percentages (i.e., less than 10%), as increased additions could dramatically alter concrete strength and durability. This paper assesses the importance of blending CWP and BFS to foster synergistic pozzolanic reactions, which would compensate the curtail in mechanical properties. Based on foregoing, the following conclusions can be drawn:

1. Regardless of binder content and  $w/b$ , the concrete mechanical properties gradually degraded when the cement is replaced by 10%–20% CWP. This was attributed to a dilution effect coupled with increased CWP porosity that detrimentally alter concrete strength and stiffness. Mixtures containing CWP exhibited higher rates of strength increase over time (compared to control mix), reflecting the pozzolanic nature of such additions.
2. Losses in the mechanical properties were remarkably reinstated when the CWP and BFS were both incorporated in the same binder, together with the cement. Hence, concrete prepared with ternary binder containing 50% cement, 15% CWP, and 35% BFS exhibited properties at 56 days comparable to the 0.54-CEM100 control mix. This practically reduces the volume of portland cement used in concrete production without impairing the performance and durability of structures.
3. The concrete toughness and modulus of elasticity decreased with CWP, given the dilution effect and intrinsic porous CWP nature that reduce stiffness and enlarge deflections for a given load. The incorporation of BFS attenuated the beam deflections during flexural testing, which was attributed to a denser microstructure achieved by synergistic pozzolanic reactions.
4. Just like the mechanical properties, the resistance to freeze/thaw cycles curtailed with CWP additions. The RDME dropped from 86% for the control CEM100 mix to 64% and down to 30% with 10% and 20% CWP rates, respectively. The CWP porous particles may have contributed to increased concrete vulnerability to water penetration and expansion under freezing conditions. The use of ternary binder improved the concrete resistance to freeze/thaw.
5. The R-value remarkably improved for concrete blocks prepared with BFS-containing binders, given the refractory nature and high MgO content of such additions. High strength concrete mixtures exhibited reduced R-values due to the reduced  $w/b$  that decreases porosity, leading to increased heat conductivity.

## Data Availability Statement

Some or all data, models, or code that support the findings of this study are available from the corresponding author upon reasonable request.

## Acknowledgments

The authors gratefully acknowledge the American University of Beirut (AUB) for supporting the research reported in this paper by the University Research Board Grant No. 103371. Also, the assistance of the staff at the CEE Materials Lab of AUB in the fabrication of the test specimens is highly appreciated.

## References

- Abdollahnejad, Z., T. Luukkonen, M. Mastali, and P. Kinnunen. 2019. "Development of one-part alkali-activated ceramic/slag binders containing recycled ceramic aggregates." *J. Mater. Civ. Eng.* 31 (2): 04018386. [https://doi.org/10.1061/\(ASCE\)MT.1943-5533.0002608](https://doi.org/10.1061/(ASCE)MT.1943-5533.0002608).
- ACI (American Concrete Institute). 2019. *Building code requirements for reinforced concrete*. ACI 318-19. Naples, FL: ACI.
- AlArab, A., B. Hamad, G. Chehab, and J. J. Assaad. 2020. "Use of ceramic-waste powder as value-added pozzolanic material with improved thermal properties." *J. Mater. Civ. Eng.* 32 (9) 04020243. [https://doi.org/10.1061/\(asce\)mt.1943-5533.0003326](https://doi.org/10.1061/(asce)mt.1943-5533.0003326).
- Aly, S. T., A. S. El-Dieb, and M. R. Taha. 2019. "Effect of high-volume ceramic waste powder as partial cement replacement on fresh and compressive strength of self-compacting concrete." *J. Mat. Civ. Eng.* 31 (2): 04018374. [https://doi.org/10.1061/\(ASCE\)MT.1943-5533.0002588](https://doi.org/10.1061/(ASCE)MT.1943-5533.0002588).
- Arora, A., G. Sant, and N. Neithalath. 2016. "Ternary blends containing slag and interground/blended limestone: Hydration, strength, and pore structure." *Constr. Build. Mater.* 102 (Jan): 113–124. <https://doi.org/10.1016/j.conbuildmat.2015.10.179>.
- Assaad, J., and C. Issa. 2014. "Effect of clinker grinding aids on flow of cement-based materials." *Cem. Concr. Res.* 63 (Sep): 1–11. <https://doi.org/10.1016/j.cemconres.2014.04.006>.
- Assaad, J., and C. Issa. 2017. "Effect of recycled acrylic-based polymers on bond stress-slip behavior in reinforced concrete structures." *J. Mater. Civ. Eng.* 29 (1): 04016173. [https://doi.org/10.1061/\(ASCE\)MT.1943-5533.0001700](https://doi.org/10.1061/(ASCE)MT.1943-5533.0001700).
- Assaad, J. J. 2017. "Influence of recycled aggregates on dynamic/static stability of self-consolidating concrete." *J. Sustainable Cem.-Based Mater.* 6 (6): 345–365. <https://doi.org/10.1080/21650373.2017.1280427>.
- ASTM. 2003. *Standard specification for concrete aggregates*. ASTM C33. West Conshohocken, PA: ASTM.
- ASTM. 2011. *Standard test method for splitting tensile strength of cylindrical concrete specimens*. ASTM C496. West Conshohocken, PA: ASTM.
- ASTM. 2012. *Standard practice for capping cylindrical concrete specimens*. ASTM C617. West Conshohocken, PA: ASTM.
- ASTM. 2014. *Standard test method for static modulus of elasticity and poisson's ratio of concrete in compression*. ASTM C469. West Conshohocken, PA: ASTM.
- ASTM. 2015a. *Standard test method for compressive strength of cylindrical concrete specimens*. ASTM C39. West Conshohocken, PA: ASTM.
- ASTM. 2015b. *Standard test method for resistance of concrete to rapid freezing and thawing*. ASTM C666. West Conshohocken, PA: ASTM.
- ASTM. 2015c. *Standard test method for slump of hydraulic-cement concrete*. ASTM C143. West Conshohocken, PA: ASTM.
- ASTM. 2017a. *Standard test method for density (unit weight), yield, and air content (gravimetric) of concrete*. ASTM C138. West Conshohocken, PA: ASTM.
- ASTM. 2017b. *Standard test method for steady-state thermal transmission properties by means of the heat flow meter apparatus*. ASTM C518. West Conshohocken, PA: ASTM.
- ASTM. 2018a. *Standard specification for slag cement for use in concrete and mortars*. ASTM C989. West Conshohocken, PA: ASTM.

- ASTM. 2018b. *Standard test method for flexural strength of concrete*. ASTM C78. West Conshohocken, PA: ASTM.
- ASTM. 2018c. *Standard test methods for sampling and testing fly ash or natural pozzolans for use in Portland-cement concrete*. ASTM C311. West Conshohocken, PA: ASTM.
- ASTM. 2019a. *Standard specification for coal fly ash and raw or calcined natural pozzolan for use in concrete*. ASTM C618. West Conshohocken, PA: ASTM.
- ASTM. 2019b. *Standard test method for fundamental transverse, longitudinal, and torsional frequencies of concrete specimens*. ASTM C215. West Conshohocken, PA: ASTM.
- Ay, N., and M. Unal. 2000. "The use of waste ceramic tile in cement production." *Cem. Concr. Res.* 30 (3): 497–499. [https://doi.org/10.1016/S0008-8846\(00\)00202-7](https://doi.org/10.1016/S0008-8846(00)00202-7).
- Aydin, S. 2008. "Development of a high-temperature-resistant mortar by using slag and pumice." *Fire Saf. J.* 43 (8): 610–617. <https://doi.org/10.1016/j.firesaf.2008.02.001>.
- CEN (European Committee for Standardization). 2011. *Cement part 1: Composition, specifications and conformity criteria for common cements*. BS EN 197/1. London: BSI.
- Deja, J. 2003. "Freezing and de-icing salt resistance of blast furnace slag concretes." *Cem. Concr. Compos.* 25 (3): 357–361. [https://doi.org/10.1016/S0958-9465\(02\)00052-5](https://doi.org/10.1016/S0958-9465(02)00052-5).
- Dieb, A. S., and D. M. Kanaan. 2018. "Ceramic waste powder an alternative cement replacement—Characterization and evaluation." *Sustainable Mater. Technol.* Sep (17) e00063. <https://doi.org/10.1016/j.susmat.2018.e00063>.
- Dieb, A. S., M. R. Taha, and S. I. Abu-Eishah. 2018. "The use of ceramic waste powder (CWP) in making eco-friendly concretes." In *Ceramic materials—synthesis, characterization, applications and recycling*. New York: IntechOpen.
- ELMir, A., S. G. Nehme, and J. J. Assaad. 2020. "Durability of self-consolidating concrete containing natural waste perlite powders." *Heliyon* 6 (1): e03165. <https://doi.org/10.1016/j.heliyon.2020.e03165>.
- Grubesa, I. N., M. J. Rukavina, and A. Mladenovic. 2016. "Impact of high temperature on residual properties of concrete with steel slag aggregate." *J. Mater. Civ. Eng.* 28 (6): 04016013. [https://doi.org/10.1061/\(ASCE\)MT.1943-5533.0001515](https://doi.org/10.1061/(ASCE)MT.1943-5533.0001515).
- Heidari, A., and D. Tavakoli. 2013. "A study of the mechanical properties of ground ceramic powder concrete incorporating nano-SiO<sub>2</sub> particles." *Constr. Build. Mater.* 38 (Jan): 255–264. <https://doi.org/10.1016/j.conbuildmat.2012.07.110>.
- Hou, J., Q. Liu, J. Liu, and Q. Wu. 2018. "Material properties of steel slag-cement binding materials prepared by precarbonated steel slag." *J. Mater. Civ. Eng.* 30 (9): 04018208. [https://doi.org/10.1061/\(ASCE\)MT.1943-5533.0002370](https://doi.org/10.1061/(ASCE)MT.1943-5533.0002370).
- Hwalla, J., M. Saba, and J. J. Assaad. 2020. "Suitability of metakaolin-based geopolymers for underwater applications." *Mater. Struct.* 53 (119): 1–14. <https://doi.org/10.1617/s11527-020-01546-0>.
- ISO (International Organization for Standardization). 2010. *Determination of the specific surface area of solids by gas adsorption—BET method*. ISO 9277. Geneva: ISO.
- Jabri, A. K., H. Shoukry, I. S. Khalil, and S. Nasir. 2018. "Reuse of waste ferrochrome slag in the production of mortar with improved thermal and mechanical performance." *J. Mat. Civ. Eng.* 30 (8): 04018152. [https://doi.org/10.1061/\(ASCE\)MT.1943-5533.0002345](https://doi.org/10.1061/(ASCE)MT.1943-5533.0002345).
- Jivkrov, A. P., D. L. Engelberg, R. Stein, and M. Petkovski. 2013. "Pore space and brittle damage evolution in concrete." *Eng. Fract. Mech.* 110 (Sep): 378–395. <https://doi.org/10.1016/j.engfracmech.2013.05.007>.
- Kannan, D. M., S. H. Aboubakr, A. S. EL-Dieb, and M. M. Taha. 2017. "High performance concrete incorporating ceramic waste powder as large partial replacement of Portland cement." *Constr. Build. Mater.* 144 (Jul): 35–41. <https://doi.org/10.1016/j.conbuildmat.2017.03.115>.
- Khayat, K., P. Trimbak, J. Assaad, and C. Jolicoeur. 2003. "Analysis of variations in electrical conductivity to assess stability of cement-based materials." *ACI Mat. J.* 100 (4): 302–310.
- Knop, Y., and A. Peled. 2018. "Sustainable blended cements—Influences of packing density on cement paste chemical efficiency." *Materials* 11 (4): 625. <https://doi.org/10.3390/ma11040625>.
- Kuan, P., Q. Hongxia, and C. Kefan. 2020. "Reliability analysis of freeze-thaw damage of recycled ceramic powder concrete." *J. Mater. Civ. Eng.* 32 (9): 05020008. [https://doi.org/10.1061/\(ASCE\)MT.1943-5533.0003360](https://doi.org/10.1061/(ASCE)MT.1943-5533.0003360).
- Lasseguette, E., S. Burns, D. Simmons, E. Francis, H. K. Chai, and V. Koutsos. 2019. "Chemical, microstructural and mechanical properties of ceramic waste blended cementitious systems." *J. Cleaner Prod.* 211 (Feb) 1228–1238. <https://doi.org/10.1016/j.jclepro.2018.11.240>.
- Lavat, A. E., M. A. Trezza, and M. Poggi. 2009. "Characterization of ceramic roof tile wastes as pozzolanic admixture." *Waste Manage.* 29 (5): 1666–1674. <https://doi.org/10.1016/j.wasman.2008.10.019>.
- Liu, D., B. Savija, G. E. Smith, P. E. J. Flewitt, T. Lowe, and E. Schlangen. 2017. "Towards understanding the influence of porosity on mechanical and fracture behaviour of quasi-brittle materials: Experiments and modelling." *Int. J. Fract.* 205 (1): 57–72. <https://doi.org/10.1007/s10704-017-0181-7>.
- Lubloy, E., K. Kopecko, G. L. Balazs, I. M. Szilagy, and J. Madarasz. 2016. "Improved fire resistance by using slag cements." *J. Therm. Anal. Calorim.* 125 (1): 271–279. <https://doi.org/10.1007/s10973-016-5392-z>.
- Malhotra, V. M. 2000. "Role of supplementary cementing materials in reducing greenhouse gas emissions." In *Concrete technology for a sustainable development in the 21st century*, 35–226. London: E&FN Spon.
- Matar, P., and J. J. Assaad. 2019. "Concurrent effects of recycled aggregates and polypropylene fibers on workability and key strength properties of self-consolidating concrete." *Constr. Build. Mater.* 199 (Feb): 492–500. <https://doi.org/10.1016/j.conbuildmat.2018.12.091>.
- Mehta, K., and P. Monteiro. 2006. *Concrete, microstructure, properties, and materials*. 3rd ed. New York: McGraw-Hill.
- Mohit, M., and Y. Sharifi. 2019. "Thermal and microstructure properties of cement mortar containing ceramic waste powder as alternative cementitious materials." *Constr. Build. Mater.* 223 (Oct): 643–656. <https://doi.org/10.1016/j.conbuildmat.2019.07.029>.
- Naciri, A., and M. C. Hamina. 2009. "Use of waste brick as a partial replacement of cement in mortar." *Waste Manage.* 29 (8): 2378–2384. <https://doi.org/10.1016/j.wasman.2009.03.026>.
- Nayana, A. M., and P. Rakesh. 2018. "Strength and durability study on cement mortar with ceramic waste and micro-silica." *Mater. Today Proc.* 5 (11): 24780–24791. <https://doi.org/10.1016/j.matpr.2018.10.276>.
- Pacheco-Torgal, F., and S. Jalali. 2010. "Reusing ceramic wastes in concrete." *Constr. Build. Mater.* 24 (5): 832–838. <https://doi.org/10.1016/j.conbuildmat.2009.10.023>.
- Quanlin, N., N. Feng, J. Yang, and X. Zheng. 2002. "Effect of superfine slag powder on cement properties." *Cem. Concr. Res.* 32 (4): 615–621. [https://doi.org/10.1016/S0008-8846\(01\)00730-X](https://doi.org/10.1016/S0008-8846(01)00730-X).
- Raval, A. D., I. N. Patel, and J. Pitroda. 2013. "Ceramic waste: Effective replacement of cement for establishing sustainable concrete." *Int. J. Eng. Trends Technol.* 4 (6): 2324–2329.
- Schlangen, E., and Z. Qian. 2009. "3D modeling of fracture in cement-based materials." *J. Multiscale Model.* 1 (2): 245–261. <https://doi.org/10.1142/S1756973709000116>.
- Schuldjakov, K. V., L. Y. Kramar, and B. Y. Trofimov. 2016. "The properties of slag cement and its influence on the structure of the hardened cement paste." *Procedia Eng.* 150 (Jan): 1433–1439. <https://doi.org/10.1016/j.proeng.2016.07.202>.
- Shi, C. 2004. "Steel slag—Its production, processing, characteristics, and cementitious properties." *J. Mater. Civ. Eng.* 16 (3): 230–236. [https://doi.org/10.1061/\(ASCE\)0899-1561\(2004\)16:3\(230\)](https://doi.org/10.1061/(ASCE)0899-1561(2004)16:3(230)).
- Siddique, S., S. Shrivastava, and S. Chaudhary. 2018. "Influence of ceramic waste as fine aggregate in concrete: Pozzolanic, XRD, FT-IR, and NMR investigations." *J. Mater. Civ. Eng.* 30 (9): 04018227. [https://doi.org/10.1061/\(ASCE\)MT.1943-5533.0002438](https://doi.org/10.1061/(ASCE)MT.1943-5533.0002438).
- Silva, J., J. de Brito, and R. Veiga. 2010. "Recycled red-clay ceramic construction and demolition waste for mortars production." *J. Mater. Civ. Eng.* 22 (3): 236–244. [https://doi.org/10.1061/\(ASCE\)0899-1561\(2010\)22:3\(236\)](https://doi.org/10.1061/(ASCE)0899-1561(2010)22:3(236)).
- Silva, R. V., J. de Brito, and R. K. Dhir. 2016. "Performance of cementitious renderings and masonry mortars containing recycled aggregates from construction and demolition wastes." *Constr. Build. Mater.* 105 (Jun): 400–415. <https://doi.org/10.1016/j.conbuildmat.2015.12.171>.

- Singh, A., and V. Srivastava. 2018. "Ceramic waste in concrete—A review." In *Proc., IEEE Int. Conf. Recent Advances on Engineering, Technology and Computational Sciences (RAETCS)*. Uttar-Pradesh, India: Sam Higginbottom Univ. of Agriculture, Technology and Sciences.
- Steiner, L. R., A. M. Bernardin, and F. Pelisser. 2015. "Effectiveness of ceramic tile polishing residues as supplementary cementitious materials for cement mortars." *Sustainable Mater. Technol.* 4 (Oct): 30–35. <https://doi.org/10.1016/j.susmat.2015.05.001>.
- Subasi, S., H. Ozturk, and M. Emiroglu. 2017. "Utilizing of waste ceramic powders as filler material in self-consolidating concrete." *Constr. Build. Mater.* 149 (5): 567–574. <https://doi.org/10.1016/j.conbuildmat.2017.05.180>.
- Sujjavanich, S., P. Suwanvitaya, D. Chaysuwan, and G. Heness. 2017. "Synergistic effect of metakaolin and fly ash on properties of concrete." *Constr. Build. Mater.* 155 (Sep): 830–837. <https://doi.org/10.1016/j.conbuildmat.2017.08.072>.
- Vejmelková, E., M. Keppert, P. Rovnaníková, M. Ondráček, Z. Keršner, and R. Černý. 2012. "Properties of high performance concrete containing fine-ground ceramics as supplementary cementitious material." *Cem. Concr. Compos.* 34 (1): 55–61. <https://doi.org/10.1016/j.cemconcomp.2011.09.018>.